数理解析研究所講究録
第830巻 1993年 1-11

密度成層流体中の物体により励起される3次元非線形内部重力波
—Navier-Stokes方程式の解と外力項を持ったKP方程式の解—

国立環境研究所　花崎秀史　(Hideshi HANAZAKI)

1.Introduction

Recent studies on the waves excited by an obstacle in the flow have revealed the basic nonlinear wave-generation mechanism. The mechanism is now found to be essentially the same for the water waves, internal gravity waves in stratified flows and for the inertial waves in swirling flows. The two-dimensional waves excited near resonance are found to be well described by the forced Boussinesq equation or the forced KdV(fKdV) equation. These model equations have been derived by Wu(1981) and Akylas(1984) for the water waves, by Grimshaw& Smyth(1986) for the internal waves, and by Grimshaw(1990) for the swirling flows. The applicability of these equations and their extensions has been verified experimentally or numerically by Lee,Yates & Wu(1989) for the water waves, by Zhu,Wu & Yates(1986), Melville & Helfrich(1987) and Hanazaki(1992) for the internal waves, and Hanazaki(1991, 1993a) for the swirling flows.

However, for the three-dimensional waves, sufficient results have not been obtained. In an experiment for the water wave, Ertekin,Webster & Wehausen(1985) found that the upstream waves become straight crested. To know the applicability of the weakly nonlinear theories, Ertekin,Webster & Wehausen(1986) solved the Green-Naghdi equation, Katsis & Akylas(1987) solved the forced KP(fKP) equation and Pedersen(1988) solved the forced Boussinesq equation. They found that, near resonance, upstream waves become two-dimensional and the generation period of the upstream wave agrees with experiments. From their results, Katsis & Akylas(1987) and Pedersen(1988) argued that the mechanism of the two-dimensionalisation is the Mach reflection of the upstream waves at the side wall of the channel. However, Tomasson & Melville(1991) solved an equation for the waves excited by a side wall perturbation in the two-layer flow. The equation is similar to the fKP equation, and with an additional assumption [see their (21)] it becomes the fKP equation. Because the solution of that equation agreed well with the solution of the linearized version of that equation when the flow is subcritical, they argued that the phenomenon can be explained by the differences in the group velocity of the lateral modes of the linear wave. Since no experimental results exist that can follow the time development of the three-dimensional patterns of the upstream wave, quantitative verification of the fKP or the forced Boussinesq equations as a time-dependent weakly nonlinear model has not been done sufficiently.

For the waves in a flow of linearly stratified Boussinesq fluid, there are a number of experiments, but none of these give three-dimensional perspective of the upstream wave. Hanazaki(1989a) has found that the upstream waves become two-dimensional by solving the three-dimensional Navier-Stokes equations. However, the channel width used was too small for the understanding of the process of the two-dimensionalisation of the upstream wave. Theoretically, Grimshaw & Yi(1991) derived a model finite-amplitude equation

for the two-dimensional resonant flow and its quantitative verification was done numerically by Hanazaki(1993b). However, corresponding theory for the three-dimensional waves are not yet developed. Because the linearly stratified Boussinesq fluid is one of the most typical type of density stratification that has been studied extensively, the investigation of its three-dimensional flow is also of much interest.

In this study, time-dependent three-dimensional Navier-Stokes equations are solved numerically. First, near resonant flow of the nearly two-layer fluid is considered. It is shown if the waves resonantly excited by an obstacle are describable by the equations derived by the weakly nonlinear theory and if the abnormal reflection similar to the Mach reflection occurs at the side wall and also if the process of two-dimensionalisation of the upstream waves can be explained by the differences in the group velocity of the lateral modes of the linear wave. In this case, the waves are expected to be governed by the fKP equation or its extensions and the comparisons with their solutions are given. Next, the results for the flow of the linearly stratified Boussinesq fluid is given.

2.Theory

The governing equations are the Navier-Stokes equations for an imcompressible stratified fluid.

$$\frac{\partial \vec{v}}{\partial t}+\left(\vec{v}\cdot\vec{\nabla}\right)\vec{v}=-\frac{1}{\rho}\vec{\nabla}p-g\hat{\vec{z}}+\frac{\mu}{\rho}\nabla^2\vec{v}, \tag{2.1a}$$

$$\frac{\partial \rho}{\partial t}+\left(\vec{v}\cdot\vec{\nabla}\right)\rho=0, \tag{2.1b}$$

$$div\vec{v}=0 \tag{2.1c}$$

where $\vec{v}$=(u,v,w) is the velocity, p is the pressure, r is the density, m is the viscosity coefficient, g is the acceleration due to gravity and $\hat{\vec{z}}$ is the unit vector along the z axis.

To derive the forced KP(fKP) equation and the forced extended KP(fEKP) equation from the inviscid form of (2.1), we rescale x,y and t as

$$X=\varepsilon^{1/2}x, Y=\varepsilon y, T=\varepsilon^{3/2}t, \tag{2.2}$$

where ε is a small parameter and expand the dependent variables in powers of ε.

At $O(\varepsilon)$, we obtain a Sturm-Liouville equation

$$\frac{d}{dz}\left(\bar{\rho}C_n^{\,2}\frac{d\phi_n}{dz}\right)-g\frac{d\bar{\rho}}{dz}\phi_n=0, \tag{2.3}$$

$$\phi_n(0)=\phi_n(D)=0, \tag{2.4}$$

where $C_n(C_1>C_2>...)$ and $\phi_n(z)$ are respectively the nth eigenvalue and the nth eigenfunction and $\bar{\rho}(z)$ is the undisturbed density.

If we scale the obstacle height h as

$$h=\varepsilon^2 H(X,Y,T), \tag{2.5}$$

we obtain the fKP equation at $O(\varepsilon^2)$, and if we consider also the effect of the cubic nonlinearity of higher order, $O(\varepsilon^3)$, we obtain the fEKP equation

$$-\frac{1}{C_n}(A_T+\Delta A_X)+a_1AA_X+\varepsilon a_2A^2A_X+a_3A_{XXX}+\frac{1}{2}\int_{-\infty}^{X}dXA_{YY}+G_X=0, \tag{2.6}$$

where

$$\Delta = \frac{U - C_n}{\varepsilon}, \tag{2.7a}$$

$$a_1 = \frac{3\int_0^D \bar{\rho}\left(\frac{d\phi_n}{dz}\right)^3 dz}{2L_n}, \tag{2.7b}$$

$$a_2 = \frac{3\int_0^D \bar{\rho}\left(\frac{d\phi_n}{dz}\right)^4 dz}{L_n}, \tag{2.7c}$$

$$a_3 = \frac{\int_0^D \bar{\rho}\phi_n{}^2 dz}{2L_n}, \tag{2.7d}$$

$$G(X,Y) = \left(\bar{\rho}\frac{d\phi}{dz}\right)_{z=0} \frac{H(X,Y,T)}{2L_n}, \tag{2.7e}$$

$$\text{and } L_n = \int_0^D \bar{\rho}\left(\frac{d\phi_n}{dz}\right)^2 dz. \tag{2.7f}$$

The fKP equation is obtained by neglecting the cubic nonlinear term $\varepsilon a_2 A^2 A_X$ in (2.6). In a two-dimensional two-layer flow, Melville & Helfrich(1987) found by experiments that the effect of the cubic nonlinearity cannot be neglected. Later, Hanazaki(1992) showed that the ratio $\varepsilon a_2/a_1$ is very large compared to the case of the water wave and the waves would be well described by the fKP equation only when the amplitude of the wave is very small. In the case of the linearly stratified Boussinesq fluid, (2.3) becomes

$$\frac{d^2\phi_n}{dz^2} - \frac{N^2}{C_n{}^2}\phi_n = 0, \tag{2.8a}$$

where the constant Brunt-Väisälä frequency is given by

$$N^2 = -\frac{g}{\bar{\rho}}\frac{d\bar{\rho}}{dz}. \tag{2.8b}$$

Therefore, $\phi_n(z)$ and C_n become

$$\phi_n(z) = \sin\frac{n\pi z}{D}, \tag{2.9a}$$

and

$$C_n = \frac{ND}{n\pi}. \tag{2.9b}$$

Substituting (2.9a) into (2.7b,f) and setting $\bar{\rho}(z)$ constant in the integrand, we know that $a_1 = 0$, which means that the quadratic nonlinear term in the fKP and the fEKP equation vanishes. In this case the nonlinear correction of the linear wave speed would be very small. This can be expected from the solution of the equation derived by Grimshaw & Yi(1991) and from the numerical solution of the two-dimensional Navier-Stokes equations [Hanazaki(1992,1993b)].

3.Numerical method

The numerical method is essentially the same as in the previous studies[Hanazaki(1989a,b),(1992)]. The computation was done in the domain of

$$x_{\min} \le x \le x_{\max}, \quad 0 \le y \le y_{\max} = W, \quad h(x,y) \le z \le z_{\max} = D, \tag{3.1}$$

where W(=40D) is the half width of the channel, D is the channel depth and the obstacle shape is given by

$$h(x,y) = h_{\max} \times \frac{1}{2}\left[1+\cos\left(\pi\left\{\left(\frac{x}{5D}\right)^2+\left(\frac{y}{10D}\right)^2\right\}^{\frac{1}{2}}\right)\right],$$

$$\text{where } \left(\frac{x}{5D}\right)^2+\left(\frac{y}{10D}\right)^2 \le 1 \tag{3.2}$$

and $h(x,y)=0$ elsewhere [$h_{\max}=0.1D$, see Figure 1].

The computation is done only for $y \ge 0$ because we assume the symmetry of the flow against the plane of $y=0$. At $y=W$ *and* $z=D$, rigid walls exist and the waves are reflected by these walls. The boundary conditions for the nearly two-layer flow are the three-dimensional counterpart of the previous studies [Hanazaki(1989a,b), (1992)].

The undisturbed density distribution $\bar{\rho}(z)$ is given by

$$\bar{\rho}(z) = \frac{1}{2}\left[\bar{\rho}(0)+\bar{\rho}(D)\right]-\frac{1}{2}\left[\bar{\rho}(0)-\bar{\rho}(D)\right]\tanh\left[\frac{50(z-h_2)}{D}\right], \tag{3.3}$$

with $\bar{\rho}(D)=0.9\bar{\rho}(0)$, and $h_2=0.3D$.

In this study, Froude number is defined by

$$F=\frac{U}{C_1}, \tag{3.4}$$

where C_1 is the maximum eigenvalue of the Sturm-Liouville problem (2.4). Specifically, in the case of the linearly stratified Boussinesq fluid, C_1 is given by (2.9b) (with n=1). The Froude number is varied as $0.6 \le F \le 1.4$. The Reynolds number is defined by

$$\mathrm{Re}=\frac{\bar{\rho}(0)Uh_{\max}}{\mu}, \tag{3.5}$$

and is fixed to be 1000.

4.Results

In Figure 2, time development of the resonant(F=1.0) flow of a nearly two-layer fluid over topography is described. Here A(x,y,t)= A_1(x,y,t) is calculated using the horizontal velocity u(x,y,z,t). In the initial time development(Ut/D=40) the upstream waves are curved backwards [Figure 2(a)]. At around Ut/D=60, the far side end of the upstream waves reaches the side wall and it begins to be reflected. After that, the upstream waves become gradually straight crested as time proceeds. Downstream of the obstacle, flat depression is formed and it becomes longer as time proceeds. Further downstream, lee waves are generated[Figure 2(d)].

To compare this solution with the weakly nonlinear theory, the solutions of the fKP and the fEKP equation [see (2.6)] when F=1.0 (Ut/D=200) are shown in Figure 3. The over all qualitative feature agree with the solution of the fully nonlinear Navier-Stokes equations. However, there are some quantitative differences. Nearly flat depression just downstream of the obstacle($x>0$, $y \cong 0$), which is typical in the two-dimensional waves and also seen in the three-dimensional solution of the Navier-Stokes equations, does not appear in the solutions of the fKP and the fEKP equation. In addition, in the solution of

the fKP equation[Figure 3(a)], the generation period of the upstream waves is shorter and the upstream-advancing speed is larger. Although the upstream waves have comparable amplitude, lee-wave amplitude is highly over predicted. In the solution of the fEKP equation[Figure 3(b)], the amplitude of the upstream wave is over predicted although the lee wave amplitude is smaller than the solution of the fKP equation. The generation period of the upstream wave is longer and the upstream-advancing speed is smaller than the solution of the Navier-Stokes equations. It seems that, except just upstream of the obstacle($x \le 0, y \le 20D$), the fEKP equation shows better agreement with the Navier-Stokes equations compared to the fKP equation. However, solution of the fEKP equation shows large differences just upstream of the obstacle($x \le 0, y \le 20D$) where we have the most concern. Therefore, we can not say straightforwardly that the fEKP equation is a sufficiently accurate model of the phenomenon. We note that, although the comparisons are made here only for F=1.0, typical qualitative differences were the same for the other Froude numbers near resonance.

To see the Froude-number dependence of the wave, results for various Froude numbers at Ut/D=200 are shown in Figure 4. When F=0.9, upstream waves are weak compared to the case of F=1.0 [Figure 2(c)]. The upstream-advancing speed is faster because of the faster linear-wave speed and the wave-generation period is shorter. The length of the downstream depression is smaller and the lee-wave amplitude is larger. When F=1.05, the upstream waves have larger amplitude and longer wave-generation period. Even when $F \ge 1$, upstream waves are generated in a long-time development as has been predicted by the weakly nonlinear theories. When F=1.1, the upstream waves have even larger amplitude but have further longer wave-generation period. When F=1.4 and the flow is supercritical, the upstream waves are no longer generated and an elevation of fluid just above the topography is trailing obliquely downstream.

A controversial issue raised here has been the mechanism of the two-dimensionalisation of the upstream wave. To see the two-dimensionalisation more clearly, the contours of A(x,y,t) corresponding to Figure 2 are shown in Figure 5. At first [Ut/D=40,Figure 5(a)], the upstream wave is curved backwards, but after the wave reaches the side wall at about Ut/D=60, the wave is reflected and a third wave whose wave crest is perpendicular to the side wall appears [Figure 5(b)]. This third wave is similar to the Mach stem that appears in the Mach reflection. The length of this third wave becomes longer as time proceeds forming a straight-crested wave front. The upstream-advancing speed of the Mach-stem like wave is faster than the wave near the center plane because the amplitude is larger. In addition, the length of the stem becomes longer roughly proportional to time. Therefore, the upstream front becomes two-dimensional as time proceeds. The amplitude of the reflected wave is very weak compared to the incident wave. Also, the angle of reflection is larger than the incident angle in Figure 5(b), (c) and (d) [see also Table 1]. These all features agree with the Mach reflection mechanism.

In Figure 6, the contours of A(x,y,t) for various Froude numbers when a short time has passed after the foremost upstream wave begins to be reflected are shown. When upstream advancing waves are generated (F=1.0,1.05 and 1.1) [see Figure 5(b),6(a,b)], the reflection angle is larger than the incident angle and the reflection pattern is qualitatively the same for all the Froude numbers near resonance($F \cong 1$). The reflection angle is consistently more than 5 degree larger than the incident angle as shown Table 1. As is typical in the Mach reflection, the amplitude of the reflected wave is weaker compared to the incident wave, although the reflection process is unsteady and the amplitude of the reflected wave is still growing in these figures. It should be noted that the Miles' theory is intended for a Boussinesq solitary wave of $\mathrm{sec}h^2$ profile. In this study, the upstream wave profile does not agree with the solution of the fKP equation and the upstream wave may not have the exact $\mathrm{sec}h^2$ profile. However, this is similar to the Boussinesq solitary wave and would show a qualitatively similar reflection pattern. When the flow is supercritical and no upstream waves are generated [F=1.4, Figure 6(c)], the

incident angle and the reflection angle agree(41°) [see Table 1] and the amplitude of the reflected wave is comparable to the incident wave. This means that the reflection is a normal reflection. Note that the wave patterns are quite similar to the solution of the forced Boussinesq equation at the same Froude number [Pedersen(1988), Figure 1(a,b)].

To see if the two-dimensionalization is a result of the linear dispersion relation, we consider the dispersion relation of the unforced linearized KP equation as done by Tomasson & Melville(1991). If we substitute

$$A(X,Y,T) \propto e^{i(kx-\omega t)} \cos\frac{l\pi y}{W}, \tag{4.1}$$

into the linearized KP equation without a forcing term [c.f.(2.6)] noting that x,y, and t are scaled as in (2.2), we obtain the dispersion relation

$$\omega = C_n\left(a_3 k^3 - \frac{l^2\pi^2}{2W^2 k}\right) + \varepsilon\Delta k. \tag{4.2}$$

To see if the linear dispersion relation can be applied to the solution of the Navier-Stokes equations, the time development of the lateral wave modes $l=0$ and $l=1$ when F=1.0 is shown in Figure 7. Because $A(x,y,t)$ can be decomposed by complete orthogonal functions as

$$A(x,y,t) = \sum_{l=0}^{\infty} \tilde{A}_l(x,t)\cos\frac{l\pi y}{W}, \tag{4.3}$$

the amplitude of the each lateral wave mode is calculated by

$$\tilde{A}_l(x,t) = \frac{2}{W}\int_0^W A(x,y,t)\cos\frac{l\pi y}{W}dy. \tag{4.4}$$

At Ut/D=200, the distance between the position of the foremost upstream wave of mode $l=0$ and $l=1$ estimeated by (4.2) is 7.2D. However, we see in Figure 7 that the propagation speed of the upstream front is almost the same in modes $l=0$ and $l=1$. In the initial time development, not only the lowest mode $l=0$ but also higher modes($l \geq 1$) are excited and propagate upstream at an equal speed. Therefore, the upstream wave is not governed by the linear dispersion relation at least near resonance. Although Tomasson & Melville(1991) showed the separation of transverse modes when F=0.6 which may be the result of the linear dispersion relation, they did not report such a separation when the flow is near resonance (F=1.05). They argued that only the lowest mode ($l=0$) can be resonant and develop nonlinearly to form two-dimensional upstream waves. However, the present solution of the Navier-Stokes equations shows that also the higher modes($l \geq 1$) develop nonlinearly and propagate upstream.

Next we consider the case of the linearly stratified Boussinesq flow. Because the two-dimensionalisation of the upstream wave has been shown also in the subcritical flow of the linearly stratified Boussinesq fluid [Hanazaki(1989a), Figure 8], it is of interest to see what occurs in these flows. As an example, we show the case of F=0.6 in Figure 8. We see the clear separation of the mode $l=0$ and $l=1$ in this case. This causes the two-dimensionalisation of the upstream wave. By assuming

$$\rho \propto e^{i(kx-\omega t)} \cos\frac{l\pi y}{W}\sin\frac{n\pi z}{D}, \text{ etc.,} \tag{4.5}$$

we can derive a dispersion relation as

$$\omega = N\left(\frac{k^2+\left(\frac{l\pi}{W}\right)^2}{k^2+\left(\frac{l\pi}{W}\right)^2+\left(\frac{n\pi}{D}\right)^2}\right)^{\frac{1}{2}}. \qquad (4.6)$$

At time Ut/D=80, the difference in the position of the foremost wave of mode $l=0$ and $l=1$ (n=1, F=0.6, W=20D) is 7.9D. The wavelength of the foremost wave of mode $l=1$ is 11.9D. These values are consistent with Figure 8. Because the upstream wave in this case is sinusoidal and not similar to the Boussinesq solitary wave, abnormal reflection similar to the Mach reflection does not occur. We know that the nonlinear correction of the linear wave speed is small in the case of the two-dimensional linearly stratified Boussinesq fluid. This would be applied also to the three-dimensional fluid. Therefore, although the propagation speed is consistent with the prediction of the linear theory, this does not mean directly that the upstream waves are governed by the linear equations.

5.Conclusion

We have found that the three-dimensional waves excited by an obstacle near resonance in nearly two-layer flow are described qualitatively by the fKP or the fEKP equation. In the process of the two-dimensionalisation of the upstream wave, it was found that the abnormal reflection similar to the Mach reflection of a Boussinesq solitary wave plays an important role. The phenomenon could not be explained by the difference in the group velocity of the lateral mode of the linear wave.

In the case of the linearly stratified Boussinesq flow, the two-dimensionalisation of the upstream wave could be explained by the difference in the group velocity of the lateral mode of the linear wave, because the upstream wave had a sinusoidal structure and the abnormal reflection that is typical to the Boussinesq solitary waves could not occur. However, this does not directly mean that the upstream waves can be described governed by the linear theory because the nonlinear correction of the linear wave speed would be very small in analogy with the results for the two-dimensional waves.

References

Akylas,T.R. 1984 J.Fluid Mech.141,455-466.

Ertekin,R.C.,Webster,W.C. & Wehausen,J.V. 1985 Proc.15th Symp. Naval Hydrodyn.

Ertekin,R.C.,Webster,W.C. & Wehausen,J.V. 1986 J.Fluid Mech.169,275-292.

Grimshaw,R.H.J. & Smyth,N. 1986 J.Fluid Mech.169,429-464.

Grimshaw,R. 1990 Studies in Appl.Math.83,249-269.

Grimshaw,R. & Yi,Z. 1991 J.Fluid Mech.229,603-628.

Hanazaki,H. 1989a Fluid Dyn.Res.4,317-332.

Hanazaki,H. 1989b Phys.Fluids A1,1976-1987.

Hanazaki,H. 1991 Phys.Fluids A3,3117-3120.

Hanazaki,H. 1992 Phys.Fluids A4, 2230-2243.

Hanazaki,H. 1993a Phys.Fluids A5 (in press).

Hanazaki,H. 1993b Phys.Fluids A5 (in press).

Kakutani,T. & Yamasaki,N. 1978 J.Phys.Soc.Japan 45,674-679.

Katsis,C. & Akylas,T.R. 1987 J.Fluid Mech.177,49-65.

Melville,W.K. & Helfrich,K.R. 1987 J.Fluid Mech.178,31-52.

Pedersen,G. 1988 J.Fluid Mech.196,39-63.

Tomasson,G.G. & Melville,W.K. 1991 J.Fluid Mech. 232,21-45.

Wu,T.Y. 1981J.Eng. Mech.Div. ASCE 107,501-522.

Zhu,J.,Wu,T.Y. & Yates,G.T. 1986 Proc.16th Symposium on Naval Hydrodyn.

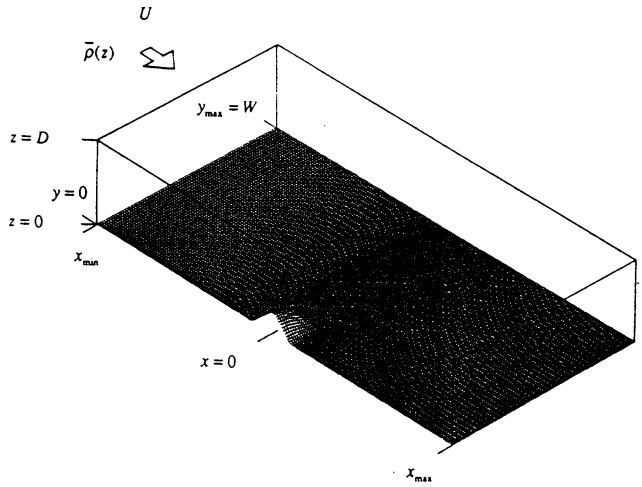

Figure 1. Schematical view of the flow geometry.

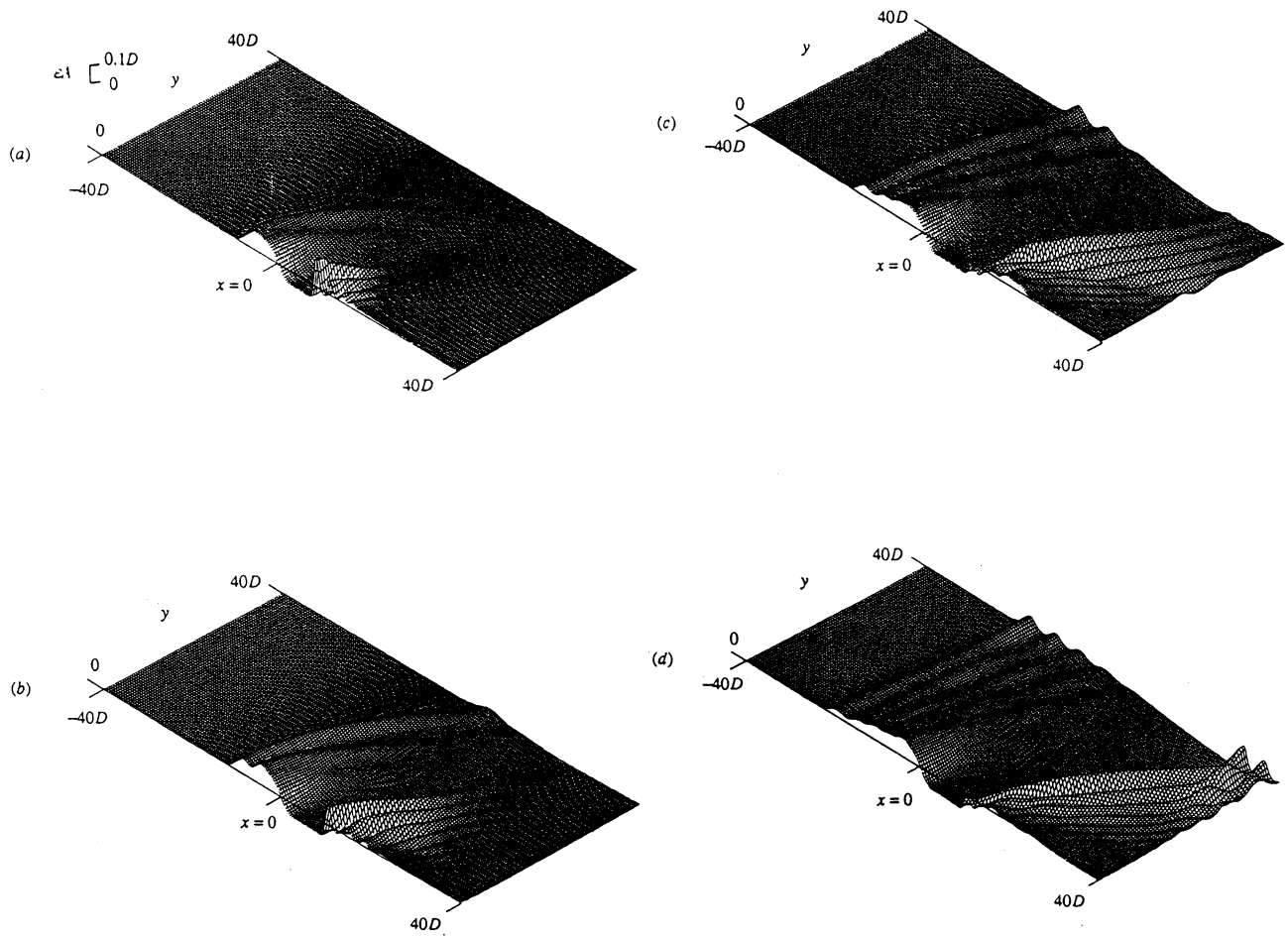

Figure 2. Time development of $A(x,y,t)$ obtained from the solution of the Navier-Stokes equations when F=1.0(two-layer flow). (a) $Ut/D = 40$; (b) $Ut/D = 80$; (c) $Ut/D = 200$; (d) $Ut/D = 400$.

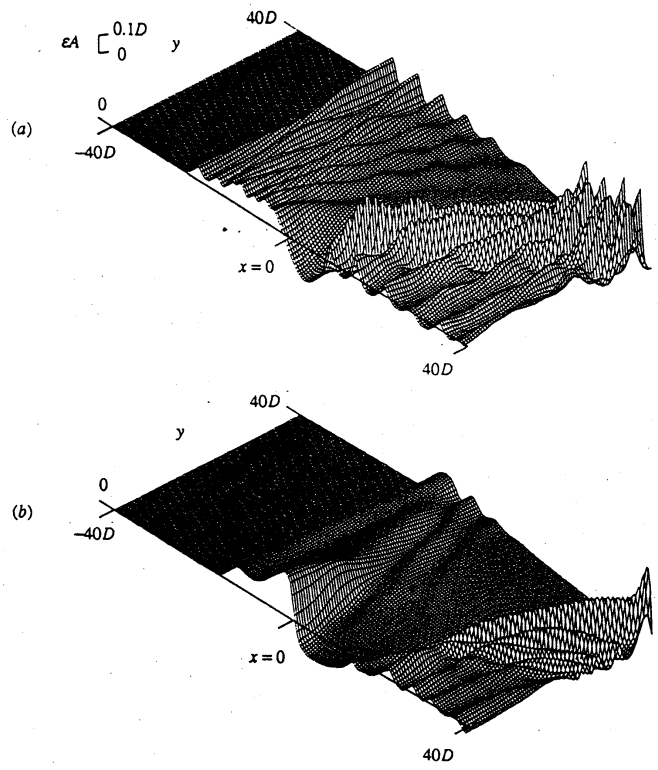

Figure 3. Time development of $A(x,y,t)$ obtained from the solution of the weakly nonlinear equations when F=1.0 (two-layer flow, $Ut/D = 200$). (a)fKP equation; (b) fEKP equation.

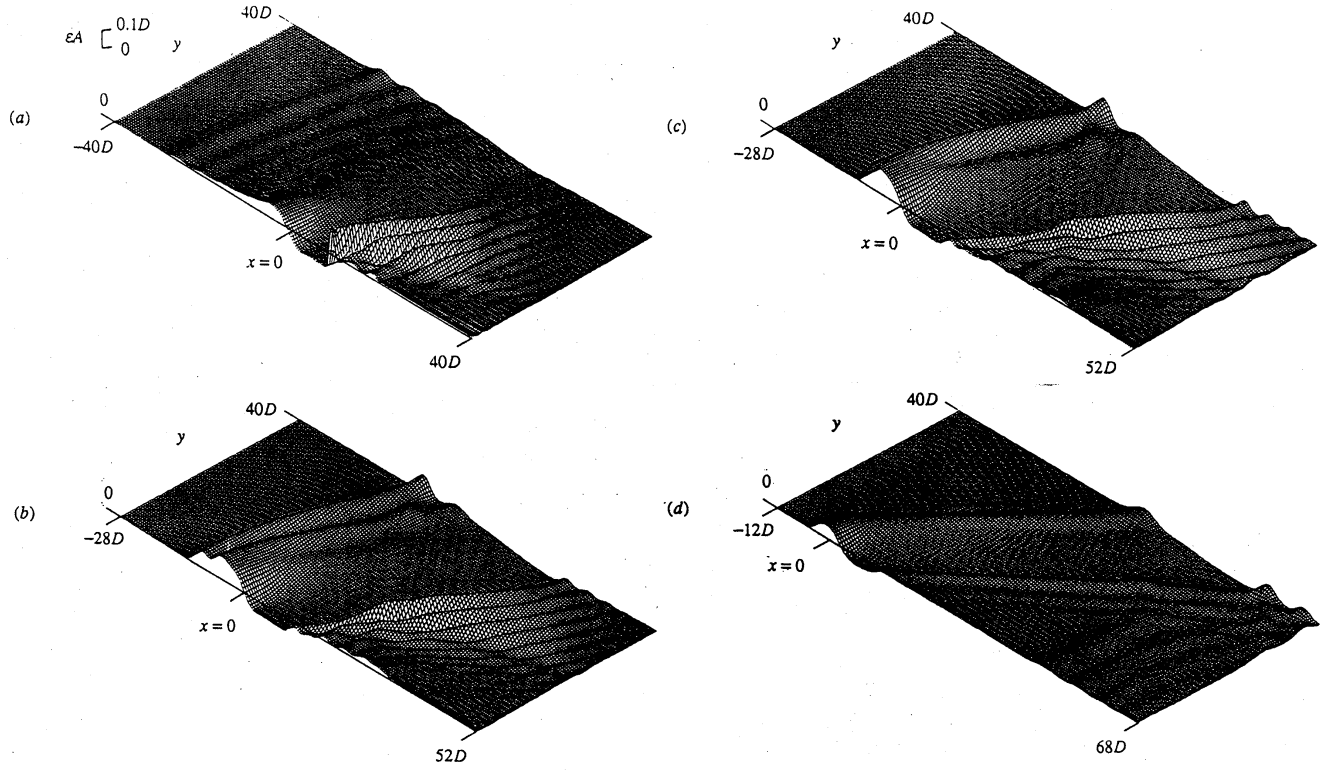

Figure 4. $A(x,y,t)$ obtained from the solution of the Navier-Stokes equations for various Froude numbers (two-layer flow, $Ut/D = 200$). (a)F=0.9; (b)F=1.05; (c)F=1.1; (d)F=1.4.

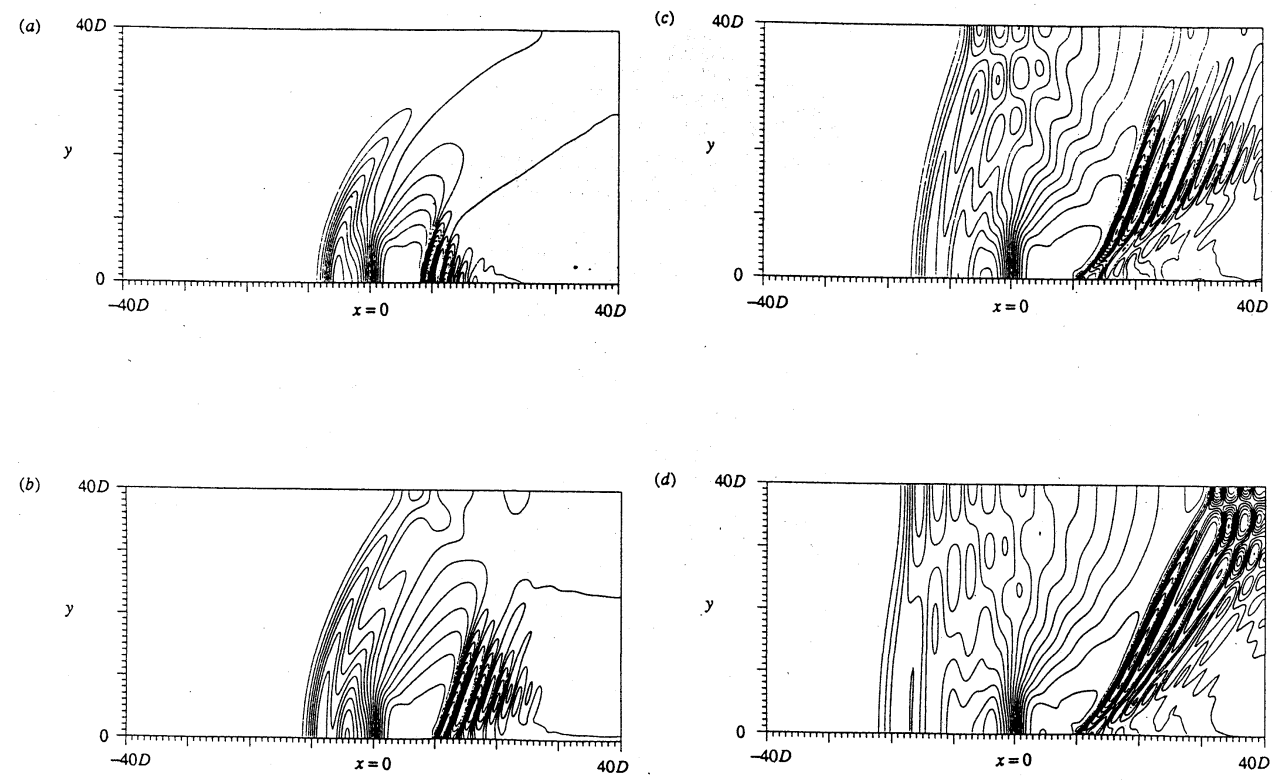

Figure 5. Time development of the contour of $A(x,y,t)$ obtained from the solution of the Navier-Stokes equations when F=1.0 (two-layer flow). (a)$Ut/D=40$; (b)$Ut/D=80$; (c)$Ut/D=200$; (d)$Ut/D=400$.

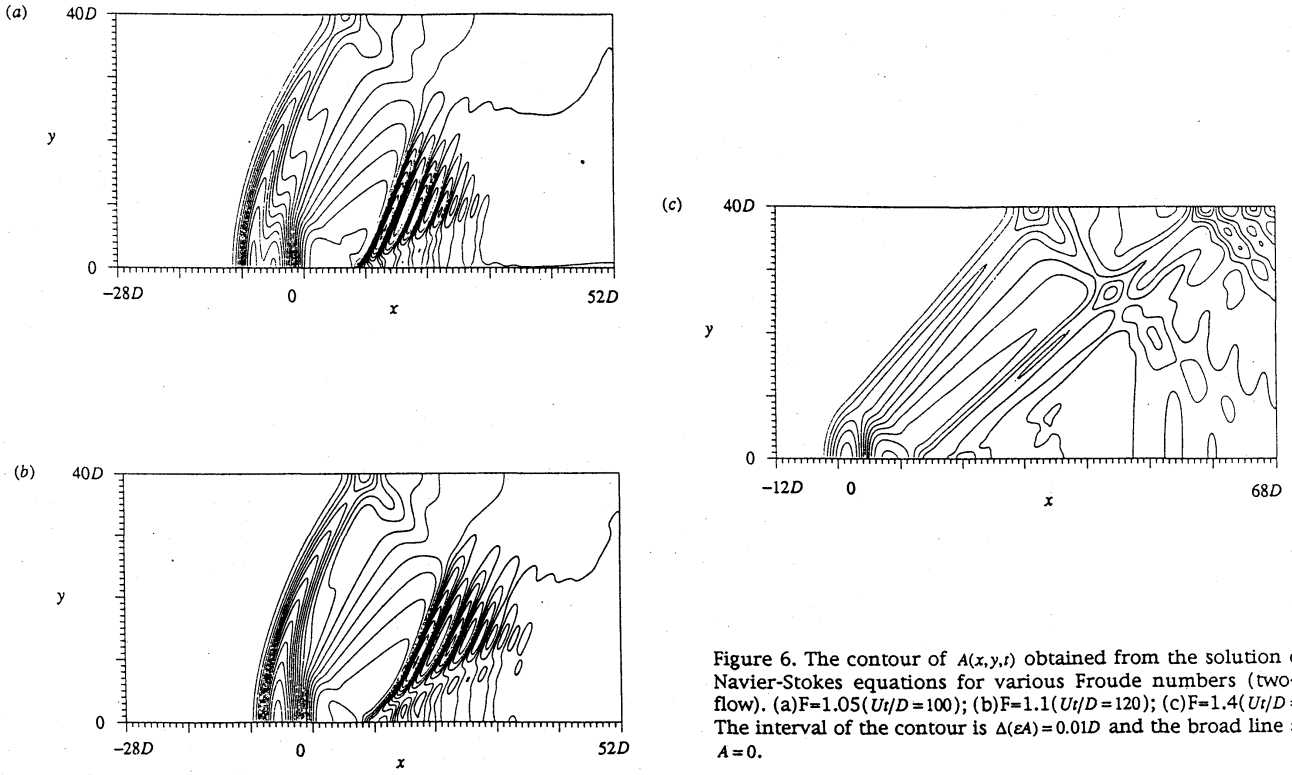

Figure 6. The contour of $A(x,y,t)$ obtained from the solution of the Navier-Stokes equations for various Froude numbers (two-layer flow). (a)F=1.05($Ut/D=100$); (b)F=1.1($Ut/D=120$); (c)F=1.4($Ut/D=200$). The interval of the contour is $\Delta(\varepsilon A)=0.01D$ and the broad line shows $A=0$.

Froude number	time (Ut/D)	channel width	incident angle (degree)	reflection angle (degree)	difference (degree)
0.6	70	20D	11	18	7
0.9	80	40D	29	36	7
1.0	80	40D	36	45	9
1.05	100	40D	33	39	6
1.1	120	40D	38	43	5
1.4	200	40D	41	41	0

Table 1. Incident and reflection angles of the upstream wave at the side wall for various Froude numbers.

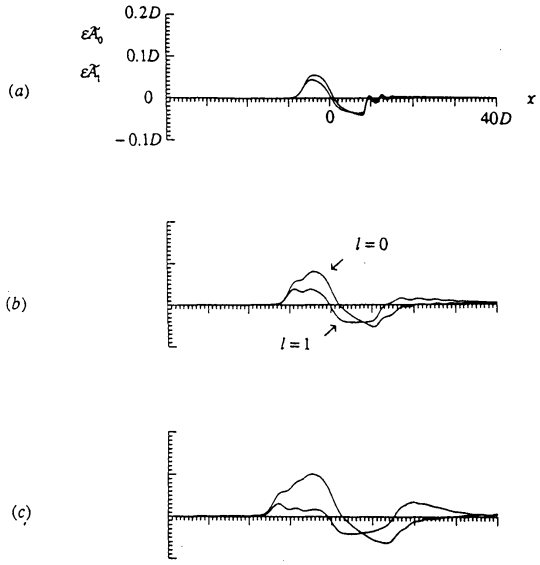

Figure 7. Time development of the lateral mode $\tilde{A}_0(x,t)$ and $\tilde{A}_1(x,t)$ in the solution of the Navier-Stokes equations when F=1.0 (two-layer flow) (a)$Ut/D = 40$; (b)$Ut/D = 100$; (c)$Ut/D = 200$.

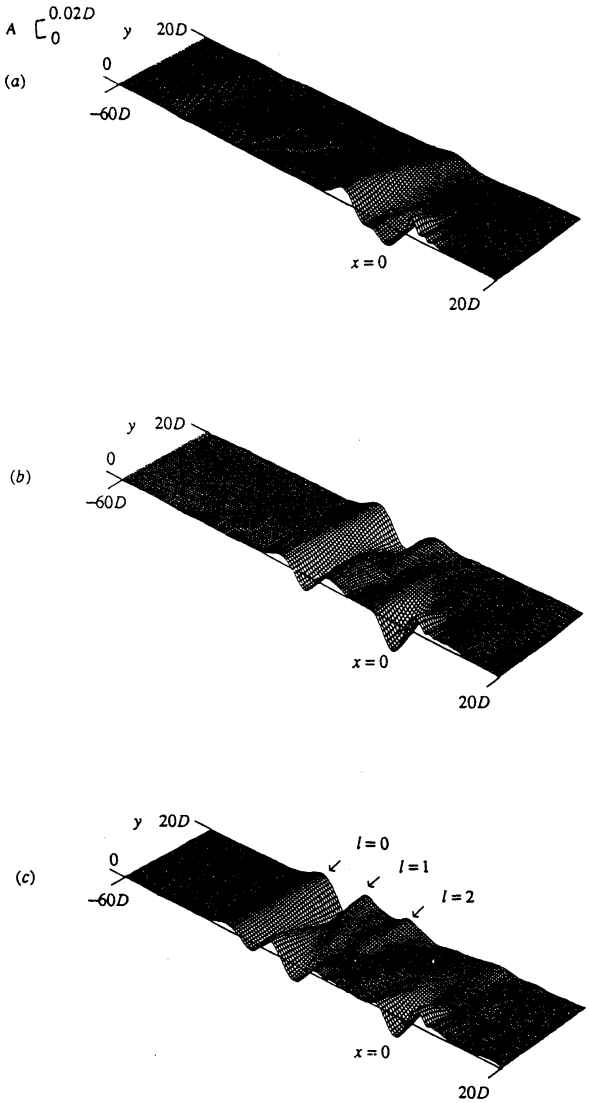

Figure 8. Time development of $A(x,y,t)$ obtained from the solution of the Navier-Stokes equations when F=0.6 (linearly stratified Boussinesq flow). (a)$Ut/D = 20$: (b)$Ut/D = 50$: (c)$Ut/D = 80$